ON FINITE ELEMENT ANALYSIS OF FRETTING FATIGUE

R. Hojjati Talemi*[1], M. Abdel Wahab[1], J. De Pauw[1]

[1]Department of mechanical construction and production, Faculty of engineering and architecture, Ghent University, 9000, Ghent, Belgium

[*] Reza.HojjatiTalemi@UGent.be

Abstract

Fretting fatigue is a combination of two complex phenomena. Fretting appears between components that are subjected to small relative oscillatory motions. Once these connected components undergo cyclic fatigue load, fretting fatigue occurs. Although several studies on fretting fatigue have been reported in literature, most of the works were of experimental nature with a Finite Element (FE) model to calculate contact stresses. There is no common standard for Finite Element Analysis (*FEA*) of fretting fatigue, despite this approach has been widely used to characterize fretting fatigue behavior. This study is focused in this direction to review the mostly used *FEA* of fretting fatigue contact models that are available in literature. A modified model is then proposed to overcome previous models' difficulties. The results indicate that the modified fretting fatigue contact model is more flexible and reliable. In this paper, after an introduction about different types of fretting fatigue FE models, some of them are simulated. Afterwards, a modified model is proposed. Finally, the contact model is validated by analytical solution and compared with available FE models.

Keywords: Fretting Fatigue, FEA

1 INTRODUCTION

Fretting fatigue is a combination of two complex phenomena. Fretting appears between components that are subjected to small relative oscillatory motion. Once these connected components undergo cyclic fatigue load, fretting fatigue occurs. Due to fretting, fatigue lifetime of components decreases significantly. There are a lot of applications that are subjected to fretting fatigue, such as bolted and riveted connections, bearing shafts, blade-disk attachment in gas and steam turbines, aero-engine splined couplings and so on [1].

Based on contact conditions, e.g. surface finish, coefficient of friction, etc, and mechanical variables, e.g. axial stress, contact stress and slip amplitude, fretting damage at contact interface can cause crack initiation and growth leading to sudden fracture. Fretting fatigue experiments have been studied by using variable type of test rigs and apparatus in different laboratories [2-7]. Either in real applications or experimental setup, it is difficult to monitor the behaviour of fretting fatigue at the contact interface, because micro-cracks and damages are always hidden between two contact components. Therefore, numerical modelling techniques such as Finite Element (FE) methods for analysing fretting fatigue are highly desirable. One of the advantages of Finite Element Analysis (*FEA*) is that it provides information, which cannot be obtained through experimental testing or analytical solution. *FEA* enables to determine local parameters in the contact region from the applied global boundary and loading conditions. Moreover, determination of these local parameters allows predictive parameters to be developed based on local rather than applied global stresses. In both the fretting fatigue's crack initiation and the early stage of crack propagation process the effect of contact stress is vital. There are enormous numerical investigations concerned with monitoring stress state at contact interface; some of them can be found in [8-11]. The majority of these models combined the *FEA* and experimental results to monitor fretting fatigue behaviour. Since there is no common standard to follow in order to model fretting fatigue, there are plenty of *FE* models available in literature.

In this paper, we try to review and categorize *FEA* of fretting fatigue in three general groups. Each of these groups represents the real application or experimental set up which is related to its practical application. Different types of *FE* models that are available in literatures are reviewed and simulated. A modified FE contact model is then proposed to cover some of difficulties of previous models.

2 CURRENT FE MODELS OF FRETTING FATIGUE

As mentioned above, are many ways to model this phenomenon due to lake of a standard guideline for *FEA* of fretting fatigue there. In this investigation, three major categories are highlighted in different groups based on recent *ASTM* standard for fretting fatigue experimental tests [12]. These three models are entitled as follows: *FEA* of practical applications, bridge-type and single clamp test.

2.1 FEA of practical applications

Some works have been modelled directly the *2D/3D* geometry of real applications such as bolted and riveted connections, shrink-fitted and dovetail- attachment joints [13-16]. Meguid et al [13] have studied a comprehensive *2D* and *3D-FEA* of the fir-tree region in aero-engine turbine disc assemblies. They have investigated the effect of the critical geometric features upon the contact stress distribution at the different teeth of a fir-tree joint. Four-node quadrilateral and Eight-node brick elements are used in their *2D* and *3D* model, respectively. They have found that 2D and *3D* results correlated well. However, the *2D* results showed the stress values by a maximum error of 10%.

Buciumeanu et al [14] have reported an investigation carried out on an automotive-formed suspension component that was subjected to fretting fatigue cyclic load. They have used tetrahedral elements for their model with quite gross mesh size of 1.8 mm at contact interface. Lanoue et al [15] have presented a *3D-FE* study of an interference fit assembly subjected to bending. They have investigated the influences of different mesh size and contact algorithms options e.g. Penalty function, Augmented Lagrange, Normal Lagrange and Pure Lagrange to evaluate stresses and strains near the contact edge where fretting fatigue failure happens. Consequently, best practice rules for interference fit *FEA* have been specified by them. Chan et al [16] have simulated a global *3D-FEA* of the disk blade assembly to examine the use of different residual compressive stress profiles to counteract the effects of contact stresses and to decrease fretting fatigue problem in engine disks. Figure 1 illustrates the full global model with different *2D* sections, which are used in their study.

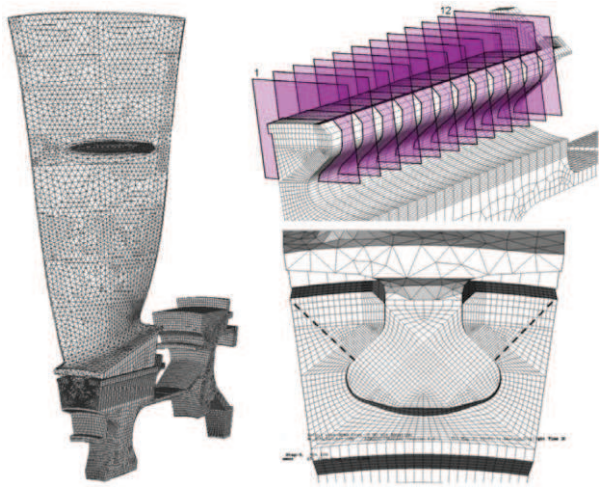

Figure 1. Blade/disk assembly, interface mesh, and *2D* zones [16]

2.2 FEA of bridge-type test

These type of fretting fatigue tests typically involve two bridge-shaped fretting pads pushing against the gage section of fatigue specimen [12]. In the lab experiments, these types of pads are not restricted to the rig's frame and are therefore free of any additional external loading. Slip at contact interface is then generated when the specimen is subjected to fatigue load. Displacement in the pad produces the tangential load transmitted to the pad at contact interface. The Schematic view of the experiments and the *FE* model for this configuration is shown in Figure 2. In most cases, only one-quarter of the test configuration is modelled due to double symmetry with respect to the *X* and *Y* axes [8, 17].

Hojjati-Talemi and Abdel Wahab [18] have investigated the effect of contact geometry on fretting fatigue crack propagation lifetime using the same approach. In their model, the four-node plane strain elements have been used along with the ‘‘master-slave’’ interfacial algorithm developed for contact modelling in the *FE* code. The Lagrange multiplier of friction have selected for contact algorithm. The loads have been applied to the *FE* model in two steps. In the first step, the contact force *F/2* has been applied to establish contact between pad and specimen. In the second step, the maximum bulk stress, σ_{max} has been applied. They have realized that in order to have accurate results, the loads must be applied in small increments due to non-linear behaviour of the contact problem. In order to have a more accurate stress distribution at the contact interface, the *FE* mesh has been refined in the contact region. The mesh refinement has been conducted until an appropriate convergence of stress state has been achieved, i.e. when the maximum stress between subsequent mesh refinements has been less than a specific amount. A difference of 5% between two consecutive steps has been used as convergence criterion.

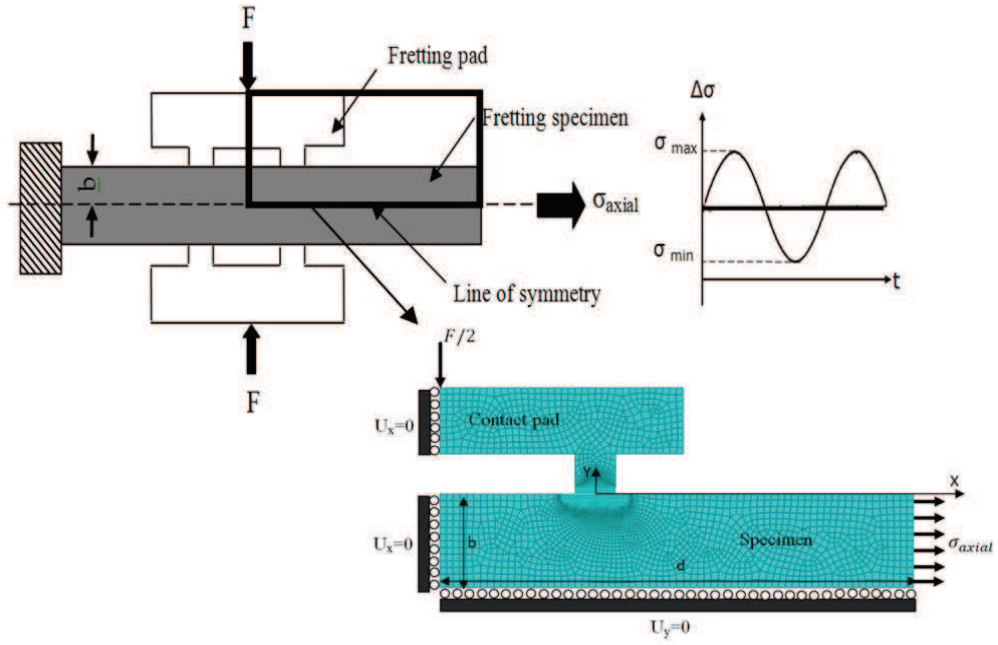

Figure 1. Schematic of experiments and *FE* model of the fretting fatigue, *b*= half thickness of specimen, *d*= half length of specimen

2.3 FEA of single clamp test

The schematic view of the single clamp test is shown in Figure 3. In contrast to the bridge-type fretting fatigue test, there is a single fretting contact at each side of fatigue specimen [12]. In this type of tests, the fretting rig is mounted on fretting fatigue apparatus in some way. Thus, the displacement amplitude at contact interface depends on the compliance of both fretting rig as well as of fatigue specimen. According to *ASTM* standard guide for fretting fatigue testing [12] there are two types of fretting rigs that allow producing tangential load at the contact interface, which are in phase with the applied bulk load to the fatigue specimen. The first type involves attached extended links to the bulk loading gripers to some points. The second type rig involves a specially designed fretting chassis that is attached to the test frame to push against fatigue experiment at both sides symmetrically [4, 12, 19, 20]. Each of these configurations has different designs from one laboratory to another one.

One of the challenging tasks in *FE* models of fretting fatigue is generating the tangential load at contact interface. As shown in Figure 3, in the second type fretting rigs, the pads are restrained by springs so that a tangential fretting force, *Q*, is applied to the contact surface in phase with the axial bulk stress. The compliance of the springs may be adjusted to ensure that $Q < \mu F$, where μ is the coefficient of friction and thus the contact remains in partial slip regime [21]. In this paper, different types of *FEA* of fretting fatigue are simulated based on some of available *FE* models in literatures.

Modelling tangential load at contact interface can be divided in two groups, namely applying direct and producing tangential load. These two groups are elaborated in the following sections. For this purpose a python script along with *FE* software, ABAQUS® [22] was employed to solve the fretting fatigue contact model shown in Figure 2.

In all simulated models, only half the experimental setup needs to be modelled using *FEA* because the experimental setup is ideally symmetric along the axial centreline of the specimen. The length and width of the specimen was *L*=20 mm and *b*=2 mm, respectively. The radius of fretting pad was considered as *R*= 50.8 mm. All of the regions had a thickness of 1 mm. A two-dimensional, 4-node (bilinear), plane strain quadrilateral, reduced integration element (*CPE4R*) was used instead of 8-noded elements (serendipity), because as it was studied by [23], the mid side node in the serendipity element causes a fluctuation in the stress state along the contact surfaces. The mesh size of 5 μm × 5 μm was considered for all models. This mesh size was gained by a mesh convergence study which will be elaborated on later. The contact between the fretting pad and the fatigue specimen was defined using the master-slave algorithm in ABAQUS® for contact between two surfaces. The circular surface of the pad was defined as a top (slave) contact surface and top surface of the specimen was defined as a bottom (master) contact surface. Both top and bottom contact surfaces were defined as a contact pair to model the possible contact region. The ABAQUS® master-slave algorithm determines which segments on the master surface and which surfaces on the slave surface interact. These master/slave surface relationships were then used to establish the contact algorithm for how loads were transferred between the two contacting surfaces. *Al* 7075-T6 was selected for both fretting pad and fatigue specimen with Modulus of Elasticity of 71.7 GPa and a Poisson's of 0.32. A Coefficient of Friction (*COF*) of 0.75 was used in this study. In all cases the normal load, maximum axial stress and tangential load ratio were considered as *F*= 40 N, $\sigma_{axial/Max}$ = 90 MPa and $Q_{max}/\mu F$ = 0.6, respectively.

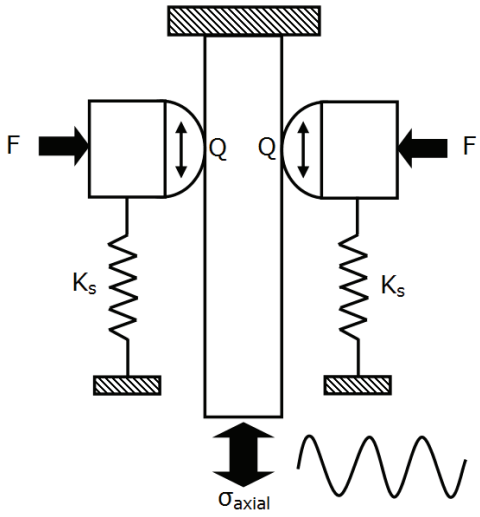

Figure 2. Schematic view of fretting fatigue experimental setup

2.3.1 Applying direct tangential load

There are numerous numerical studies that have applied directly tangential load to the fretting pad in order to simulate the experiment's configuration [9, 10, 24-26]. This approach can be divided in two categories as summarised below.

a. With fretting pad holder

The *FE* model consisted of three reigns: the fatigue specimen, the fretting pad and fretting pad holder. In these models, a plate with low modulus of elasticity is attached to the side of the fretting pad, which is called pad holder [9, 10, 24, 25]. The primary purpose of the fretting pad holder in the *FE* model is to restrain the pad in the *X* and *Y* directions prior to the application of load. Therefore, the stiffness of the pad holder should be low to have a minimal effect on the interaction between the fretting pad and fatigue specimen.

As the geometry and loading conditions are indicated in Figure 4, the specimen was fixed at its far end in the negative *X*-direction, restricted from vertical movement along its bottom surface and free to roll in the *X*-direction and along its bottom edge. The cylindrical pad is rigidly fixed to the pad holder with the pad holder being free to roll in the y-direction along the side opposite to the fretting pad. Multi-Point Constraint (*MPC*) was also applied at the top of fretting pad as well as the border between fretting pad and holder in order to prevent it from rotating due to the application of loads. As it is mentioned above the material properties of the pad holder differ from the other two reigns. An Elastic Modulus and a Poison's Ratio of 0.03 MPa and 0.3 were then signed to the pad holder respectively. Finally, the loads were applied in two steps: First the normal load *F* was applied and then held constant. In the second step, the maximum tangential and axial applied stress was applied simultaneously.

b. With restricted fretting pad

Massingham and Irving [27] tried to model the second type of experimental configuration which is explained above, with attached extended links to the bulk loading gripers to some points. In this study their model was used to model the same material and loading conditions, but with different boundary conditions. As it is illustrated in Figure 5, the boundary +conditions for fatigue specimen are the same as the previous model. The pad holder was eliminated from the *FE* model and the right side of pad was restricted in *X*-direction but free to roll in the *Y*-direction. Furthermore, normal and shear load was applied at top and left side of pad, respectively.

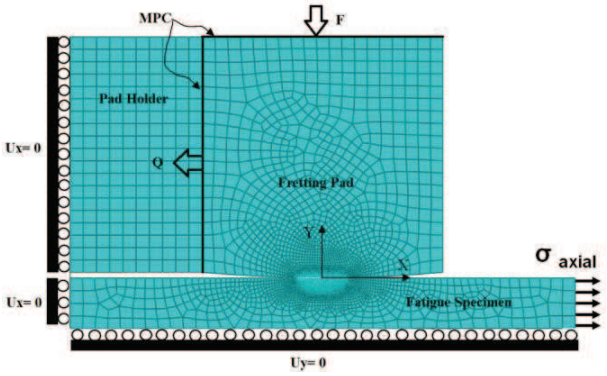

Figure 3. FE model with fretting pad holder

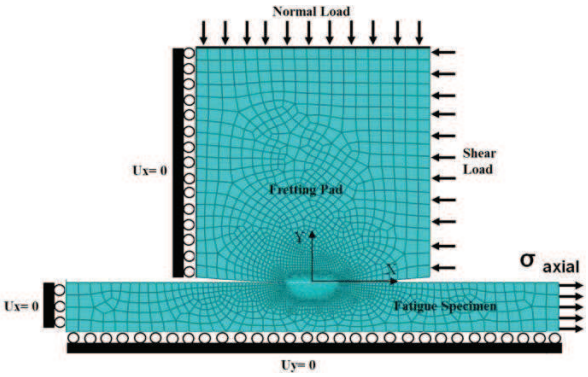

Figure 5. FE model with restricted pad

2.3.2 Producing tangential load

In contrast to some models that have directly applied tangential load to the fretting pad, some of researchers have tried to generate tangential load at contact interface between fretting pad and fatigue specimen [25, 28-30]. These models can be simulated in different ways. In this paper two ways that are mostly used in literatures are explained and finally the modified *FEA* of fretting fatigue is purposed.

a. Attached spring or beam

One of the possibilities in order to generate tangential load is adding a spring or beam element at the right side of the fretting pad as depicted in Figure 6. The sequence of applying the normal and axial load is the same as in previous models, just because of the frictional contact and the way the pad is supported, a tangential load *Q* is generated on the fretting pad. The magnitude of the tangential load and the bulk stress on the left part of the specimen depend on the compliances of both the specimen and the fretting pad support (attached spring). Giner et al [29] and H-Gangaraj et al [30] have represented these compliances in their model by attaching spring and beam element of stiffness K_s, respectively. Also, they have used *MPC*s to guarantee an even distribution of point forces over the fretting pad top and right side.

b. Applying displacement

In some studies the tangential load has been produced by applying displacement on fretting pad [28]. This type of models was also simulated in this study to compare with other models. Figure 7 indicates the boundary and loading conditions of this model. From the figure, the sequence of applying normal

and axial load is the same as mentioned above. Both sides of fretting pad as well as top of pad are restricted using *MPC* to prevent it from rotating due to the application of displacement, also to guarantee an even distribution of point forces over the fretting pad top. The magnitude of displacement was based on tangential load which is applied at right side of pad. In order to find accurate displacement amplitude, *Q* was applied to right side of fretting pad to measure the related displacement that should be applied to generate the same tangential load. This step was not part of *FE* model and was just modeled to find the displacement amplitude instead of experimental measurements.

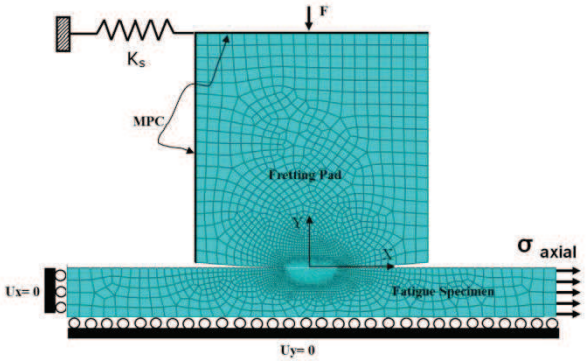

Figure 6. FE model with attached spring

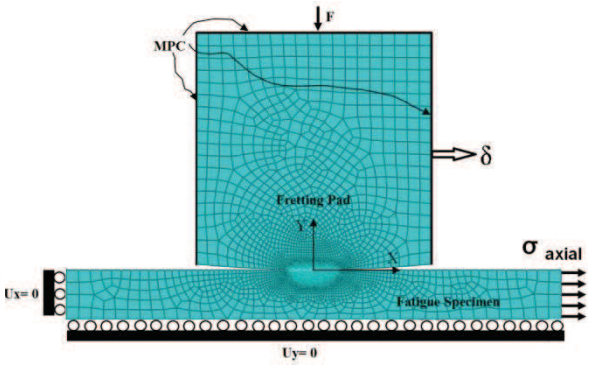

Figure 7. FE model with applied displacement

c. Proposed modified model

In this study, a modified approach was used to simulate the fretting fatigue contact model. As illustrated in Figure 8, both sides of fretting pad were restricted to move only vertically. The MPC was also applied at the top of pad in order to avoid it from rotating due to the application of loads. The loads were applied in two steps. Normal contact load, *F*, was applied in the first step to establish contact between the pad and the specimen. In this modified model for applying tangential load *Q*, the experimental data was used. In experimental tests, the tangential force is defined by subtraction of the axial bulk load and the reaction load that can be measured by an attached load cell to the fixed side of specimen. Then by dividing it by two, the tangential load at each side of specimen, which is in contact with fretting pad, was obtained as:

$$Q = \frac{F_{axial} - F_r}{2} \tag{1}$$

Where F_{axial} is the axial bulk load and F_r is the axial reaction load. In order to model the effect of attached spring to the fretting pad for generating tangential load, the reaction stress (σ_R) can be calculated based on equation 2, where A_s is cross section area of specimen as shown in Figure 8:

$$\sigma_R = Q \times A_s - \sigma_{axial} \tag{2}$$

Therefore, in the modified model, in the second step, the maximum axial stress σ_{axial} and the reaction stress σ_R were applied at the same time at right and left sides of specimen, respectively, to match the experimental maximum cyclic loading condition.

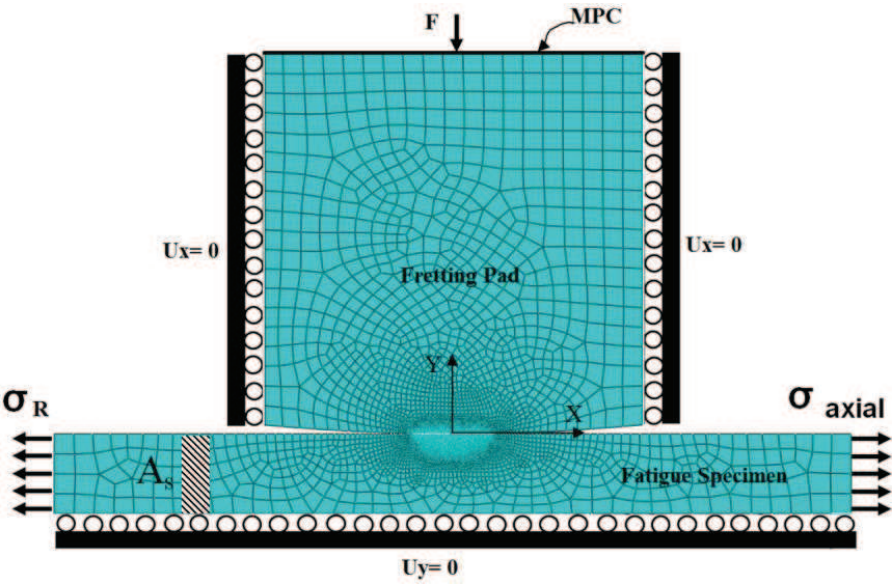

Figure 8. Modified FE model of fretting fatigue

3 VALIDATION OF FE MODEL

In order to validate the proposed modified model two steps were carried out. First, a mesh convergence study was carried out to find the appropriate mesh size at contact region between fretting pad and fatigue specimen. Since the stress components near the contact region are high and their distributions are quite complex, a very fine mesh was used in this region. The mesh refinement was conducted until an appropriate convergence of stress state was achieved. The proper mesh size was gradually increased in the regions far from the contact interface. Analytical solution was then used to validate *FE* stress distribution at contact interface.

3.1 Mesh convergence study

The mesh size at contact interface should be fine to capture the relaxed stress state near the leading and trailing edges, i.e. the leading edge is near to the side where axial stress was applied and the trailing edge is near to the clamped side of the specimen. The modelling with mesh refinement was continued until an appropriate convergence of the stress state was achieved, i.e. when the maximum stress between subsequent mesh refinements was less than a specific amount. In this investigation, a difference of 1.57% between the two consecutive steps was used as the convergence criterion, which was defined as follows:

$$e = \left| \frac{\sigma_{max}^{i+1} - \sigma_{max}^{i}}{\sigma_{max}^{i+1}} \right| \times 100 \tag{3}$$

Where e is the convergence parameter, σ_{max}^{i} is the maximum stress in i^{th} model and σ_{max}^{i+1} is the maximum stress in $(i+1)^{th}$ model. According to mesh convergence study that is shown in figure 9, an acceptable element size was determined to be at least 5 μm × 5 μm in the refined contact zone. Jayaprakash et al [17] have reported the relationship between tangential stress at the contact edge and mesh size for a bridge type pad with sharp corners. From their observation they have found that there was a transition in slope at a mesh size of 5 μm the stress became much sensitive to mesh size when the mesh size was smaller than 5 μm. However, they could not find a logical reason for this transition behaviour. The minimum mesh sizes used for contact problems were in the range of 5–50 μm [10, 24, 28, 31-33] as listed in table 1.

Table 1. Fretting fatigue contact mesh size

Reference	Minimum mesh size at contact interface (μm)
Hojjati et al [31]	5
Madge et al [28]	6
Iyer and Mall [24]	6.2
Nishida et al [32]	10
Bernardo et al [33]	20
Tsai and Mall [10]	50

Figure 9 shows the variation of tangential stress (σ_{xx}) using different element sizes at the contact interface for cylindrical fretting pad. Figure 10 indicates the variation of maximum tangential stress at contact interface at location of *x/a* = 1. It is interesting to note that for cylindrical pad the behaviour was not the same as reported by Jayaprakash et al [17]. This result confirms that in both cases of bridge type and cylindrical pad there is transition in slop. For bridge type pad the slop is at a mesh size of 5 μm and for cylindrical pad is at 15 μm. Furthermore, the attentions can be drawn to singular behaviour of fretting fatigue contact in both the bridge type and the cylindrical fretting pad.

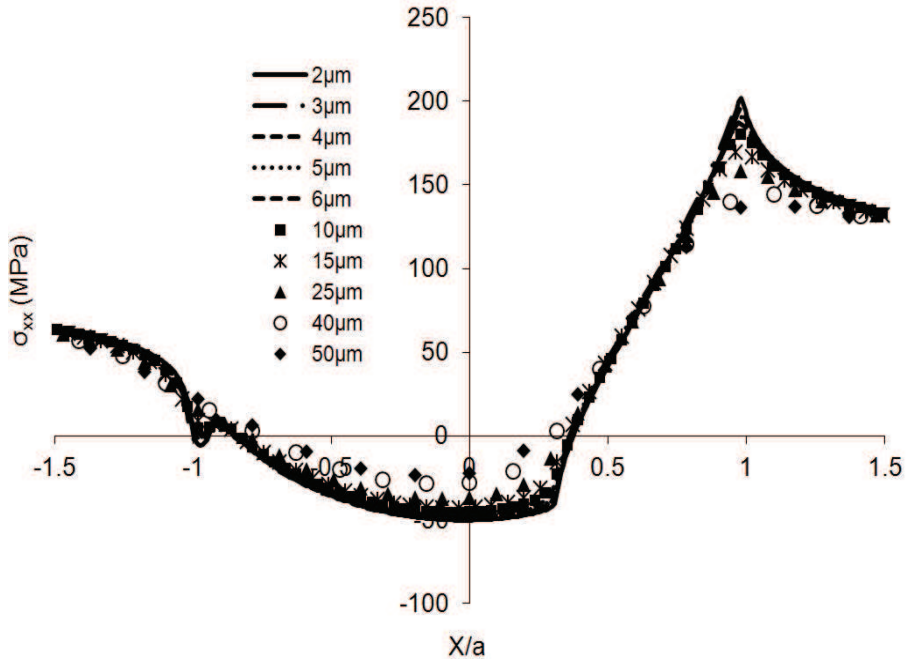

Figure 9. Convergence of tangential stress σ_{xx} at contact interface

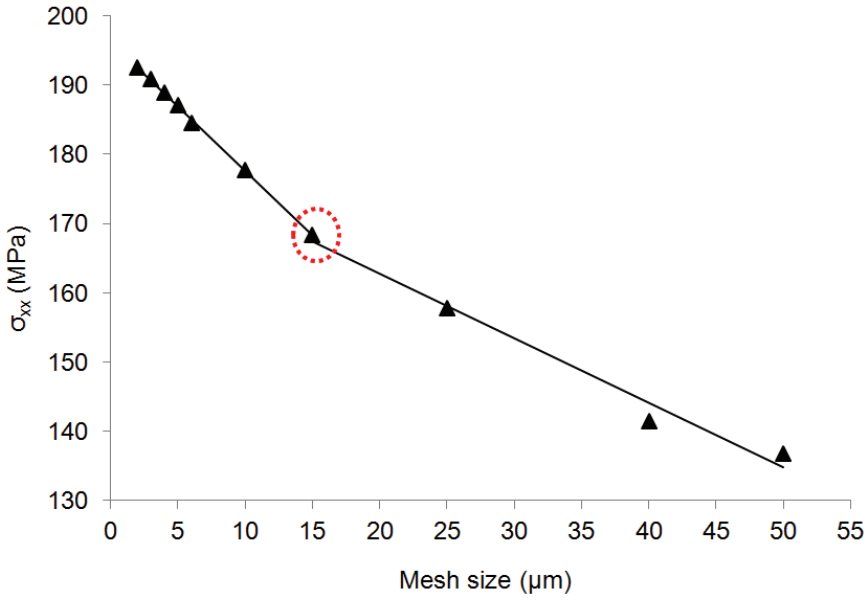

Figure 10. Relationship between tangential stress σ_{xx} at contact edge and mesh size

3.2 Comparing with analytical solution

When two elastically similar bodies are brought into normal contact the resulting displacement of adjoining points on the two bodies are the same when a normal load, *F*, is applied to one of the bodies. The solution to the ensuing pressure distribution, *F(x,y)*, is called the Hertz solution. The Hertz solution states that there will be a peak stress at the middle of the contact surface. For the case of a fretting pad in contact with the fatigue specimen, it is possible to solve for the pressure distribution when the assumptions of the Hertz solution are met. The primary assumptions are that the radii of both bodies are large relative to the contact dimensions and that the contacting bodies have infinite boundaries. The assumption that the bodies have infinite boundaries is commonly referred to as the Half Space assumption.

The Half Space assumption is considered to be met and the boundaries can be considered infinite if one half of the fatigue specimen thickness, *b*, is equal to or greater than ten times the contact half width, *a*, or in other words *b/a* > 10. Fellows et al. [19] found that a finite dimension of *b/a* = 3 results in stress in the *X*-direction increasing by as much as 20% at the edge of contact due to the applied normal and tangential load. Therefore, violation of the infinite boundary assumption can cause significant deviation from the analytical solution. Consequently, for comparing numerical results with analytical solution two assumptions were considered: a) the elastic behaviour of material and b) the ratio of *b/a* = 7.84. For the square mesh with 5 μm at contact region, the *FEA* contact half width, *a*, varied by 0.39% between *FEA* and analytical results [21], where a_{FEA} = 255 μm and $a_{analytical}$ = 254 μm. The predicted maximum Hertzian pressure, P_o, by the FE model was in good agreement with the analytical solution with a 0.25% difference; $P_{o\text{-}FEA}$ = 100.3 MPa versus $P_{o\text{-}Analytical}$ = 100.052 MPa. Figure 11 depicts the frictional shear stress distribution over contact region for both analytical solution and *FE* model with element size of 5 μm. The figure shows good correlation between calculated and predicted frictional shear stress. Therefore, as mentioned above the same mesh size was utilized for all simulated *FE* models.

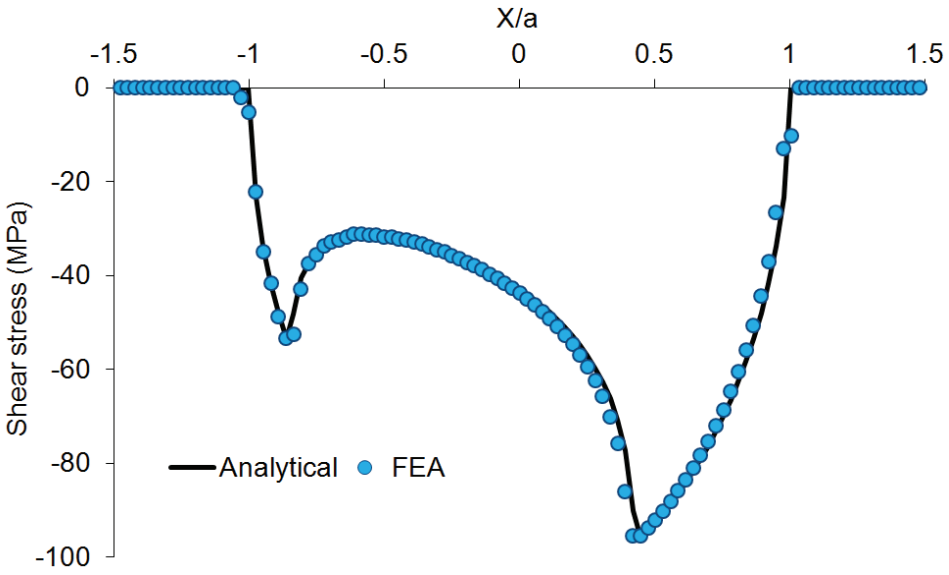

Figure 11. The comparison of frictional shear stress between analytical and numerical results at surface nodes (F= 40 N, σ_{axial} = 90 MPa, $Q/\mu p_0$= 0.6 N, μ= 0.75, R= 50.8 mm)

4 COMPARING DIFFERENT FE MODELS OF FRETTING FATIGUE

In this section some of the models that are explained above for single clamp experimental testes are compared together. According to the explanation that is given in section 2 these models can be named as follows: Applied Q-with pad holder (Figure 4), Applied Q-with restricted pad (Figure 5), Applied displacement (Figure 7) and the proposed modified model (Figure 8). Figure 12 indicates the variation of σ_{xx} over the contact interface for these models. As it can be seen, there is a good correlation between all models except the model that used by Massingham and Irving [27]. According to authors believe, this big difference comes from the constraint that was applied at the right side of fretting pad. This constraint restricted the pad to move in X-direction, therefore, all stress distributions at the contact region would be affected by this constraint. To overcome this difficulty the boundary conditions of this model were modified. Both sides of fretting pad were restricted to move in X-direction while the normal load was applied. These constraints were inactivated and *MPC* was added to the left side pad when the axial load was applied. As it is shown in the Figure 12, these changes have led to right stress distribution at the contact interface. Also, a slight deviation can be seen at the trailing edge of contact, which in particular can be related to the value of Elastic Modulus of pad holder and the displacement that was applied to pad.

Figure 13 illustrates the σ_{xx} distribution in depth of 2 mm of fatigue specimen at x/a =1. This graph reveals that despite a slight difference between σ_{xx} stress that was distributed over the contact interface, the tangential stress distributions at x/a =1 beneath the contact line was completely matched for different models that were simulated in this study.

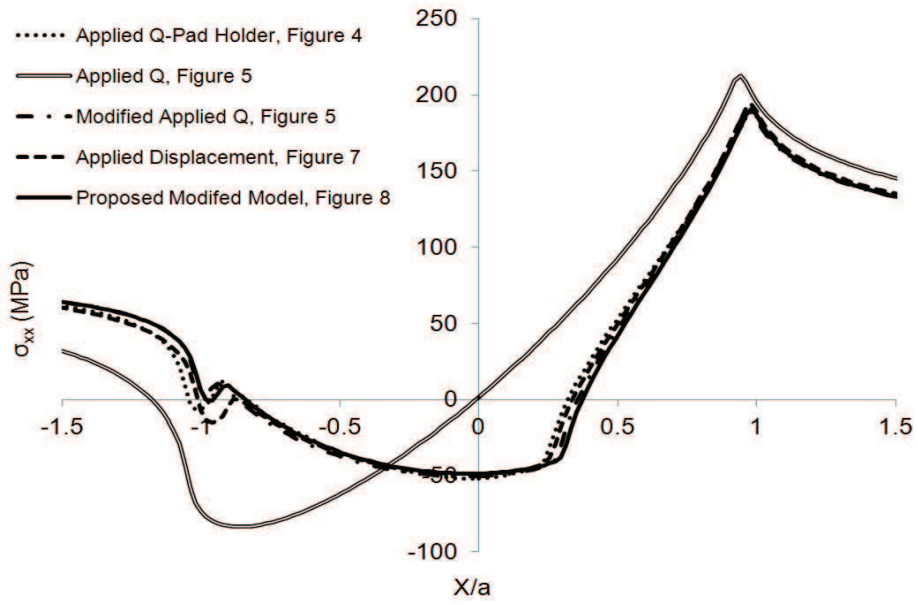

Figure 12. Compression between different *FE* models of fretting fatigue

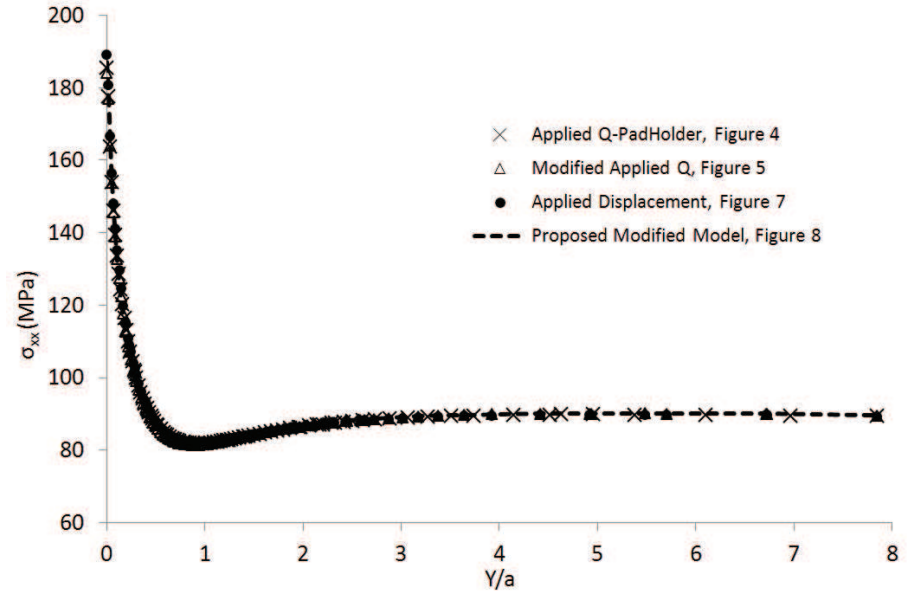

Figure 13. Compression of tangential stress σ_{xx} distribution in depth of 2 mm of fatigue specimen at *x/a* =1 for different *FE* models of fretting fatigue

4 DISCUSSION

As mentioned above modelling the tangential load at contact interface is a challenging task. In this study different types of *FEA* of fretting fatigue were simulated based on some of available finite *FE* models in literatures. Each of these models that are available in literatures has some disadvantages that might cause some problems for *FEA* of fretting fatigue. The issues related to these models are discussed in this section.

Applying Q-with pad holder (Figure 4): In this model the compliance of fretting pad holder with the experimentally measured *Q* was a challenging issue. In particular in order to model different tangential loads the Elastic Modulus of attached plate to the pad should be updated using trial and error process. It means that in each experimental test using different loading condition, first the *FE* model should be validated.

Applying Q-with restricted pad (Figure 5): As mentioned above, this type of model does not show a good response to different loading conditions. At least for loading conditions that were used in this study, it does not correlate with other models as shown in the figure 12. This big deviation might be related to the constraint that was applied at the right side of fretting pad. This constraint restricted pad to move in *X*-direction, therefore, all stress distributions at the contact region would be affected by this constraint.

Attached spring or beam element (Figure 6): In these models, the tangential load was generated based on the stiffness of attached spring or beam element. The same problem for the model with pad holder can be extended to these models. The compliance difficulty of this type of models can be seen in the *FE* model of H-Gangaraj et al [30].

Applying displacement (Figure 7): According to Figure 12 this type of model shows good correlation to analytical solution. The main problem of this model is the value of displacement that should be applied to the pad. The displacement amplitude can be measured using the experimental setup, for instance Sabelkin and Mall [34] measured relative slip from experiments between a location on fretting pad and a location on fatigue specimen.

The difference between the modified *FE* model (*Figure 8*) and the previous models is that, in the modified model the pad is restricted to move in *X*-direction. Instead of pad, specimen is moved to produce the tangential load (*Q*) at contact interface. In all cases the tangential load causes the same stress distribution at contact surface. But, the proposed modified *FE* model is simple and reliable. Furthermore, the modified model does not need the compliance with the type of fretting fixture that is used in experimental tests. The proposed modified model just needs the value of tangential load that should be applied at contact interface which can be easily calculated based on experimental tests regardless of type of fretting fatigue apparatus.

5 CONCLUSION

In this paper, fretting fatigue experimental configurations are reviewed and categorized in three general groups. Each of these groups represents the real application or experimental set up, which is related to its practical application. Different type of *FE* models that are available in literatures are reviewed and simulated. Finally, a modified *FE* model is proposed to cover some of difficulties of previous models. From this study it can be concluded that the same as fretting fatigue experimental tests it is crucial to have standard guide for *FEA* of fretting fatigue. In most cases the *FE* models are used to characterize fretting fatigue and are further implemented to predict fretting fatigue crack initiation and propagation lifetime. Therefore, as an important step, the *FE* model should be accurate enough and it is not acceptable to build a structure on a shaky foundation.

As future work this idea can be extended to have a standard guideline for *FEA* of fretting fatigue which might covers the below aspects.

1- Geometrical design, e.g. bridge type or single and double clamped tests.
2- Contact algorithm, e.g. Penalty function, Augmented Lagrange, Normal Lagrange and Pure Lagrange.
3- Contact properties, e.g. node or surface to surface, finite or small sliding.
4- Fretting slip amplitude, e.g. partial slip and gross slip.
5- Mesh convergence study, e.g. minimum mesh size at contact region.
6- Validation criteria, e.g. half-space specimen's rules.
7- Loading and boundary conditions.

Also, other details, which can be considered as a general *FEA* parameter of fretting fatigue model.

6 ACKNOWLEDGEMENTS

The authors wish to thank the Ghent University for the financial support received by the Special Funding of Ghent University (Bijzonder Onderzoeksfonds), in the framework of *BOF* project (BOF 01N02410).

8 REFERENCES

[1] Hills, D.A., Nowell, D., Mechanics of fretting fatigue, Kluwer Academic Publisher, 1994.
[2] M.P. Fatigue Crack Nucleation, in: Proceedings of 1995 USAF Structural Integrity Program Conference, San Antonio, TX, 237-265, 1995.
[3] Szolwinski, M.P., Farris, T.N., Mechanics of fretting fatigue crack formation, Wear, 198, 93-107, 1996.
[4] Szolwinski, M.P., Farris, T.N., Observation, analysis and prediction of fretting fatigue in 2024-T351 aluminum alloy, Wear, 221, 24-36, 1998.
[5] Jin, O., Mall, S., Effects of slip on fretting behavior: experiments and analyses, Wear, 256, 671-684, 2004.
[6] Arora, P.R., Jacob, M.S.D., Salit, M.S., Ahmed, E.M., Saleem, M., Edi, P., Experimental evaluation of fretting fatigue test apparatus, International Journal of Fatigue, 29, 941-952, 2007.
[7] Majzoobi, G.H., Hojjati-Talemi R., Nematian, M., Zalnejad, E., Ahmadkhani, A.R. and Hanifepoor, E., A new device for fretting fatigue testing, Transactions of the Indian Institute of Metals, 63 (2-3), 493-497, 2010.
[8] Mutoh, Y., Xu, J.-Q., Fracture mechanics approach to fretting fatigue and problems to be solved, Tribology International, 36, 99-107, 2003.
[9] Wang, R.H., Jain, V.K., Mall, S., A non-uniform friction distribution model for partial slip fretting contact, Wear, 262, 607-616, 2007.
[10] Tsai, C.T., Mall, S., Elasto-plastic finite element analysis of fretting stresses in pre-stressed strip in contact with cylindrical pad, Finite Elements in Analysis and Design, 36, 171-187, 2000.
[11] Jayaprakash, M., Mutoh, Y., Yoshii, K., Fretting fatigue behaviour and life prediction of automotive steel bolted joint, Materials & Design, 32, 3911-3919, 2011.
[12] ASTM, Strandard guide for fretting fatigue testing, in, ASTM, USA, 1-10, 2011.
[13] Meguid, S.A., Kanth, P.S., Czekanski, A., Finite element analysis of fir-tree region in turbine discs, Finite Elements in Analysis and Design, 35, 305-317, 2000.
[14] Buciumeanu, M., Miranda, A.S., Pinho, A.C.M., Silva, F.S., Design improvement of an automotive-formed suspension component subjected to fretting fatigue, Engineering Failure Analysis, 14, 810-821, 2007.
[15] Lanoue, F., Vadean, A., Sanschagrin, B., Finite element analysis and contact modelling considerations of interference fits for fretting fatigue strength calculations, Simulation Modelling Practice and Theory, 17, 1587-1602, 2009.
[16] Chan, K.S., Enright, M.P., Moody, J.P., Golden, P.J., Chandra, R., Pentz, A.C., Residual stress profiles for mitigating fretting fatigue in gas turbine engine disks, International Journal of Fatigue, 32, 815-823, 2010.
[17] Jayaprakash, M., Mutoh, Y., Asai, K., Ichikawa, K., Sukarai, S., Effect of contact pad rigidity on fretting fatigue behavior of NiCrMoV turbine steel, International Journal of Fatigue, 32, 1788-1794, 2010.
[18] Hojjati-Talemi, R., Abdel Wahab, M., Numerical investigation into effect of contact geometry on fretting fatigue crack propagation lifetime, Tribol. Trans., To appear 2012.
[19] Fellows, L.J., Nowell, D., Hills, D.A., Contact stresses in a moderately thin strip (with particular reference to fretting experiments), Wear, 185, 235-238, 1995.
[20] Murthy, H., Rajeev, P.T., Okane, M., Farris, T.N., Development of test methods for high temperature fretting of turbine materials subjected to engine-type loading, in: Mutoh, Y., Kinyon, S.E., Hoeppner, D.W., (Eds.) Fretting Fatigue: Advances in Basic Understanding and Applications, American Society Testing and Materials, W Conshohocken, 273-288, 2003.
[21] Hills, D.A., Nowell, D., Mechanics of fretting fatigue, Kluwer Academic Publishers, Dordrecht ; Boston, 1994.
[22] ABAQUS /Standard 6.11 User's Manual, in: K.a.S. Hibbit, Providence, Rhode Island (Ed.).
[23] Lykins, C., An Investigation of Fretting Fatigue Crack Initiation Behavior of the Titanium Alloy Ti-6Al-4V, in, University of Dayton 1999.
[24] Iyer, K., Mall, S., Analyses of contact pressure and stress amplitude effects on fretting fatigue life, J. Eng. Mater. Technol.-Trans. ASME, 123, 85-93, 2001.
[25] Ding, J., Houghton, D., Williams, E.J., Leen, S.B., Simple parameters to predict effect of surface damage on fretting fatigue, International Journal of Fatigue, 33, 332-342, 2011.
[26] Shin, K.-S., Kim, G.W., A study on the prediction of fretting fatigue behavior, Procedia Engineering, 10, 665-670, 2011.

[27] Massingham, M., Irving, P.E., The effect of variable amplitude loading on stress distribution within a cylindrical contact subjected to fretting fatigue, Tribology International, 39, 1084-1091, 2006.
[28] Madge, J.J., Leen, S.B., McColl, I.R., Shipway, P.H., Contact-evolution based prediction of fretting fatigue life: Effect of slip amplitude, Wear, 262, 1159-1170, 2007.
[29] Giner, E., Tur, M., Vercher, A., Fuenmayor, F.J., Numerical modelling of crack-contact interaction in 2D incomplete fretting contacts using X-FEM, Tribology International, 42, 1269-1275, 2009.
[30] H-Gangaraj, S.M., Alvandi-Tabrizi, Y., Farrahi, G.H., Majzoobi, G.H., Ghadbeigi, H., Finite element analysis of shot-peening effect on fretting fatigue parameters, Tribology International, 44, 1583-1588, 2011.
[31] Hojjati-Talemi, R., Abdel Wahab, M., De Baets, P., De Pauw, J., Effect of different fretting fatigue primary variables on relative slip amplitude, Mechanical engineering letters, 5, 57-67, 2011.
[32] Nishida, T., Kondoh, K., Xu, J.Q., Mutoh, Y., Observations and analysis of relative slip in fretting fatigue, in: Mutoh, Y., Kinyon, S.E., Hoeppner, D.W., (Eds.) Fretting Fatigue: Advances in Basic Understanding and Applications, American Society Testing and Materials, W Conshohocken, 33-43, 2003.
[33] Bernardo, A.T., Araújo, J.A., Mamiya, E.N., Proposition of a finite element-based approach to compute the size effect in fretting fatigue, Tribology International, 39, 1123-1130, 2006.
[34] Sabelkin, V., Mall, S., Investigation into relative slip during fretting fatigue under partial slip contact condition, Fatigue Fract. Eng. Mater. Struct., 28, 809-824, 2005.

